N76 14540

Solar Flux and Its Variations

ELSKE V. P. SMITH AND DAVID M. GOTTLIEB
University of Maryland

We present data on the solar irradiance as derived from a number of sources. An attempt was made to bring these data onto a uniform scale. The results are presented in table 5 and figure 6. Summation of fluxes at all wavelengths yields a figure of 1357.826 for the solar constant. Estimates are made of the solar flux variations due to flares, active regions (slowly varying component), 27-day period, and the 11-yr cycle. Solar activity does not produce a significant variation in the value of the solar constant. Nevertheless, variations in the X-ray and EUV portions of the solar flux may be several orders of magnitude during solar activity, especially at times of major flares. It is, of course, well established that these short wavelength flux enhancements cause significant changes in the terrestrial ionosphere.

This paper is intended to be a review of what we know about the photon flux from the Sun at all wavelengths, and its variations. The emphasis has been placed on determining values for the solar constant (total electromagnetic energy flux from the Sun incident on Earth); the solar irradiance (wavelength distribution of the flux), of use to workers in the geophysical-meteorological field; and the variation of the irradiance as a function of solar activity. Accordingly, emissions shorter than 2 Å and longer than 2 cm have been ignored, as the total energies involved are exceedingly low.

We shall begin with a review of the general nature of the solar spectrum. At radio and IR wavelengths (10 000 Å to 2 cm), the solar spectrum is essentially a continuum, with the bulk of the emission occurring from progressively higher regions in the solar atmosphere at the longer wavelengths. Below 10 000 Å, occasional absorption lines appear superimposed on a photospheric continuum, becoming more and more numerous as we go toward the UV. Around 5000 Å, about 10 percent of the continuum flux is blocked by lines; near 3500 Å, about 40 percent. The continuum flux drops off sharply below 4000 Å, but the fraction of the energy absorbed in lines remains high until about 2100 Å. Here, a sharp decrease in continuum flux occurs, coincident with the A1(I) ionization edge, and the absorption lines all but disappear. The photospheric continuum flux continues to drop off, and emission lines begin to appear around 1750 Å. The last absorption lines die out near 1500 Å, and the photospheric continuum itself dominates over the emission lines only until 1300 to 1400 Å. At shorter wavelengths, chromospheric and coronal emission lines dominate until the coronal continuum begins to make itself felt below 100 Å. From 2 to 100 Å, one finds a mixture of continuum and lines—both are coronal in origin. Special mention should be made of the extremely strong Lyman-alpha emission line of H(I) at 1216 Å. The flux from just this line usually exceeds the combined flux from all shorter wavelengths.

In the next section we discuss the solar spectrum of the quiet Sun in detail and in the final section we investigate variations, especially in X-ray and UV emissions, caused by flares, plages, and other effects.

THE QUIET SUN

Flux Versus Specific Intensity

Two types of measurements of solar radiation are commonly made: the flux from the entire disk

and the specific intensity measured over a small area at the center of the disk.

The quantity we need is the solar irradiance (the solar flux at 1 AU), which can be derived directly from the total solar flux according to the equation

$$H = \pi \frac{r^2}{R^2} F$$
$$= 6.80 \times 10^{-5} F$$

where H is the solar irradiance, and r is the radius of the Sun, R is 1 AU, and F is the total solar flux. We use the units W/m² · Å to specify H.

Converting specific intensity to solar irradiance requires knowledge of the limb darkening at each wavelength. Such data are not always available, especially in the far UV. We have deduced limb darkening values at many wavelengths below 1800 Å where direct observational data are very incomplete.

Once limb darkening is known, the flux can be calculated by

$$F = \frac{1}{\pi} \int I(0) L(\theta) \cos \theta \, dw$$

where I(0) is the specific intensity at the center of the disk, $L(\theta) = I(\theta)/I(0)$ is the limb darkening, and θ is the angle viewed from the Sun's center between the sub-Earth point and position on the disk.

The Visible Region: 3300 to 10 000 Å

In the wavelength region 3300 to 10 000 Å, we adopt the data of Labs and Neckel. They made specific intensity measurements of over 100 20-Å bandpasses at Jungfraujoch during 1961 to 1964 (Labs and Neckel, 1967). The authors estimate their errors to be everywhere less than about 1 percent. Labs and Neckel (1968) later combined their data with limb darkening data from David and Elste (1962) to obtain the solar irradiance in 100-Å bands. Finally, Labs and Neckel (1970) report a minor revision to transform their values to the International Practical Temperature scale of 1968, incorporating the revised value of the melting point of gold. (It should be noted that there is an error in the caption to table 7 of Labs and Neckel, 1970, in that the units given should read μW/cm².)

Other observations of the solar flux at visible wavelengths have been made, for example, by Arvesen et al. (1969), Drummond et al. (1968); see also Laue and Drummond (1968). The Labs and Neckel data are in good agreement with most of these observations; further, they marshall very good arguments in favor of their values, based on reanalyses of previous data. Moreover, the Labs and Neckel results are almost precisely identical to the Willstrop (1965) data for the G^2V star HD 20766. For these reasons, we have adopted the Labs and Neckel data from 3300 to 10 000 Å.

Near Infrared: 10 000 to 24 000 Å

The Labs and Neckel data end at 12 000 Å; for longer wavelengths we rely on measures by Arvesen et al. (1969) and Pierce (1954).

Pierce's data are on a relative scale, but the absolute calibration was provided by Labs and Neckel (1968). The scaling was done by adjusting Pierce's data to the models of Gingerich et al. (1971) and Holweger (1967).

When the data were plotted (see fig. 1), it became clear that they could be fit with a series of straight lines of the form.

$$\log F = \alpha + \beta \text{ long } \lambda$$

where F is the irradiance in W/m²Å, λ is the wavelength in Å, and α and β are listed in table 1.

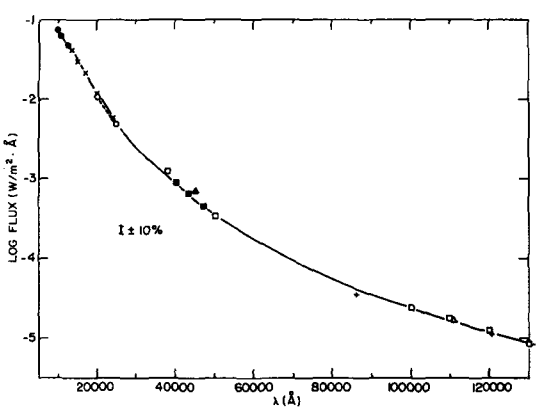

FIGURE 1.—The solar flux in the IR. (Filled circles: Labs and Neckel, 1968; x: Arvesen et al., 1969; open circles: Pierce, 1954; open squares: Koutchmy and Peyturaux, 1970; filled squares: Murcray, 1969; filled triangles: Farmer and Todd, 1964; plus signs: Saiedy, 1960; open triangle: Saiedy and Goody, 1959.)

Longer Wavelengths: 25 000 Å to 2 cm

Above 25 000 Å, data have been taken from several sources. Farmer and Todd (1964) used spectra to get one datum point at 45 000 Å. Koutchmy and Peyturaux (1970) report measurements from the Pyrenees Mountains for seven wavelengths from 38 000 to 200 000 Å. Murcray et al. (1964) have balloon data for 40 000 to 50 000 Å, and Saiedy and Goody (1959), and Saiedy (1960) report three measurements near 100 000 Å. The gap between the far IR and the radio region is bridged by four data points from Eddy et al. (1969), who used a NASA aircraft for their observations. Linsky (1973) has published a compendium and recalibration of work from 0.1 to 2 cm and then derived a mean relation. In many cases the data are given as a brightness temperature, but this can be converted to irradiance by

$$H = \frac{8.09 \times 10^{-21}}{\lambda^5 (e^{1.44/\lambda T} - 1)}$$

where H is the irradiance in W/m² · Å, λ is the wavelength in cm, and T is the brightness temperature in K.

The data are presented in figure 2. Once again, they can be fit with straight line segments.

Near Ultraviolet: 2100 to 3300 Å

For this spectral region we adopt the Broadfoot (1972) rocket data. Unfortunately, his data extend only from 2100 to 3200 Å, with the last 100 Å being rather uncertain. The Labs and Neckel (1968, 1970) data extend down only to 3300 Å. To bridge this gap, and to determine if the two sets of data are consistent, we use the Arvesen et al. (1969) data from 3000 to 3300 Å, first scaling these data by a factor of 0.87 to get them to the Labs and Neckel scale. Table 2 presents the results. The scaled Arvesen data points from 3100 to 3300 Å have been adopted. For 3000 to 3100 Å, the agreement of the data is very encouraging, and so for wavelengths shorter than 3100 Å, we use Broadfoot's data.

Far Ultraviolet: 1400 to 2100 Å

In this region of the spectrum, the absorption lines fade out, emission lines begin, but the photospheric continuum dominates the flux.

TABLE 1.—*Coefficients for the Linear Relation Between Log Flux and Log Wavelength*

Wavelength range	α	β
10 000 to 12 460 Å	7.670	−2.198
12 460 to 15 000 Å	8.702	−2.450
15 000 to 24 000 Å	13.026	−3.485
24 000 to 40 000 Å	13.820	−3.667
40 000 to 50 000 Å	15.781	−4.093
50 000 to 100 000 Å	14.736	−3.870
100 000 to 200 000 Å	15.534	−4.030
0.02 to 0.238 mm	15.291	−3.984
0.238 to 0.312 mm	15.828	−4.068
0.312 to 1.0 mm	13.510	−3.711
1.0 to 3.0 mm	14.297	−3.824
3.0 to 10.0 mm	13.598	−3.730
10.0 to 20.0 mm	12.991	−2.654

TABLE 2.—*Various Values of the Solar Irradiance in the UV*

Wavelength range, Å	Solar irradiance, W/m² · 100Å	
	Arvesen et al. (1969)[a]	Broadfoot (1972)
3000 to 3100	5.09	5.18
3100 to 3200	6.35	5.82
3200 to 3300	7.81	—

[a] Scaled to the Labs and Neckel data.

Relatively good intensities are available from 1400 to 1900 Å from Bruckner and Nicolas (1973), Rottman (1973) as quoted in Donnelly and Pope (1973), and Parkinson and Reeves (1969). We prefer these data to the higher values obtained by Bonnet and Blamont (1968) and Widing et al. (1970). The adopted lower values, besides being very self-consistent, yield a value of 4400 K for the temperature minimum, which agrees with IR data. Further, Carver et al. (1972) report on some 50 Å resolution data from WRESAT I ion chambers, which are also in good agreement with the adopted data. We used the Bonnet and Blamont limb darkening curves together with values derived from Dupree and Reeves (1971) data to convert the intensities to irradiances. Figure 3 depicts the data and the limb darkening (F/I) values used.

Above 1900 Å we have less reliable data. We use the shape, but not the absolute calibration, of the Bonnet and Blamont (1968) and Widing et al. (1970) data and scale them to fit both figure 3 and Broadfoot's (1972) data. The very abrupt

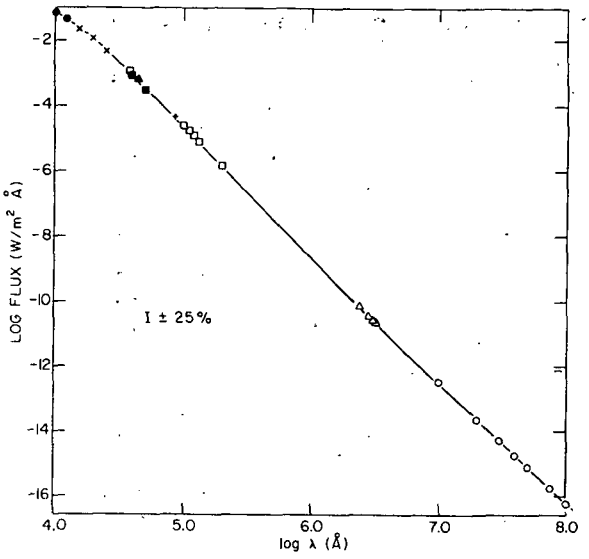

FIGURE 2.—Solar irradiance in the microwave region. The solid line is the adopted fit. (Filled circles: Labs and Neckel, 1968; x: Arvesen et al., 1969; open squares: Koutchmy and Peyturaux, 1970; filled squares: Murcray, 1969; filled triangles: Farmer and Todd, 1964; plus signs: Saiedy, 1960; open triangles: Eddy et al., 1969; open circles: Linsky, 1973.)

rise in flux from 2075 to 2100 Å, shown in figure 6, is real. This corresponds to the A1(I) ionization edge and appears clearly in spectra.

Extreme Ultraviolet: 500 to 1400 Å

Below 1400 Å, the solar spectrum is dominated by chromospheric and coronal emission lines. Contributions are also made by the continua of C(I), H(I), and He(I).

Virtually all available data are from the OSO satellites. Irradiance values come from OSO 3 (Hall and Hinteregger, 1970) and OSO 4 (Reeves and Parkinson, 1970). Specific intensities from OSO 6 (Dupree et al., 1973) are available for more lines and probably at better accuracy. Dupree and Reeves (1971) have some additional specific intensities from OSO 4.

Because we wish to base our evaluation on the OSO 6 data, some knowledge of limb darkening is necessary. Fortunately, the effect is small for most lines (Noyes and Kalkofen, 1970; Withbroe, 1970*a, b*). However, for some high ionization potential lines, there is limb brightening.

To evaluate *F/I*, we have compared the OSO 6

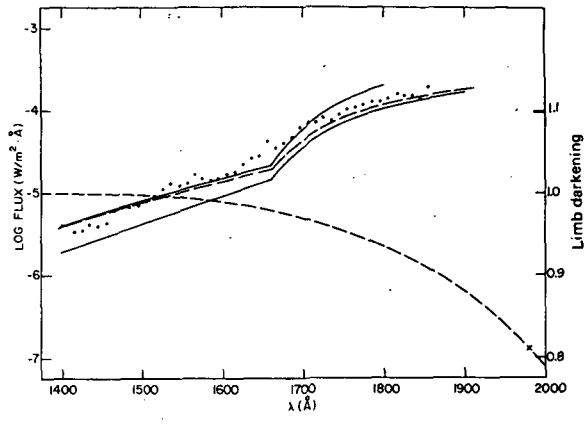

FIGURE 3.—Solar irradiance in the UV. The dash line is the adopted limb darkening. The dots are from Rottman (1973); the upper solid line is from Nicolas (1973); the lower solid line is from Parkinson and Reeves (1969); and the dash line between the two is the adopted limb darkened solar irradiance.

data to the fluxes from Reeves and Parkinson (1970). Here *I* is defined as the flux as if there were no limb effect; *F/I* is a function of ionization potential (IP) and wavelength. (See table 3.)

Table 4 presents the irradiances for each line. We made allowance for the continua of C(I), H(I), and He(I), as well as a correction to allow for the extended wing of H(I) (wavelength equal to 1216 Å). The data used were from Dupree and Reeves (1971). The H(I) (wavelength equal to 1216 Å) line is by far the strongest present. A profile of the line is given by Bruner and Rense (1969).

Soft X-Rays: 2 to 500 Å

The coronal continuum contributes significantly to the total solar flux below 100 Å, but from 100 to 500 Å the flux comes almost entirely from emission lines.

What is meant by "quiet" Sun becomes a critical consideration at these wavelengths. In general, a "quiet" Sun would have a sunspot number of

TABLE 3.—*Values for Limb Darkening*

Wavelength, Å	*F/I, eV*
800 to 1400	1.201 + 0.0114IP
600 to 800	1.350 + 0.0068IP
500 to 600	1.069 + 0.0014IP

TABLE 4.—*Ultraviolet Emission Lines and Their Strengths During Moderate Solar Activity*

Wavelength, A	Ion	Irradiance, W/m²	Wavelength, A	Ion	Irradiance, W/m²
468	—	1.9 (−6)	790	O(IV)	9.9 (−6)
469	Ne(IV)	5.7 (−7)	834	O(II), O(III)	1.7 (−5)
476	—	8.8 (−8)	859	—	1.5 (−6)
482	Ne(V)	6.2 (−7)	904	C(II)	5.2 (−6)
489	Ne(III)	1.4 (−6)	923	N(IV)	6.4 (−6)
499	Si(III)	7.5 (−6)	931	H(I)	4.8 (−6)
507	O(III)	3.7 (−6)	933	S(VI)	2.9 (−6)
515	He(I)	8.8 (−7)	937	H(I)	6.1 (−6)
521	Si(XII)	5.6 (−6)	944	S(VI)	1.8 (−6)
525	O(III)	1.6 (−6)	949	H(I)	9.0 (−6)
537	He(I)	4.1 (−6)	959	—	3.9 (−7)
542	Ne(IV)	7.7 (−7)	973	H(I)	1.8 (−5)
550	Al(XI)	5.1 (−7)	977	C(III)	1.4 (−4)
554	O(IV)	1.0 (−5)	988	—	6.2 (−6)
559	Ne(VI)	9.3 (−7)	991	N(III)	9.2 (−6)
562	Ne(VI)	1.1 (−6)	1010	C(II)	1.8 (−6)
568	Al(XI), Ne(V)	6.3 (−7)	1021	S(III)	1.3 (−6)
572	Ne(V)	6.5 (−7)	1025	H(I)	6.8 (−5)
580	O(II)	7.0 (−7)	1031	O(VI)	4.7 (−5)
584	He(I)	3.2 (−5)	1037	O(VI)*	4.2 (−5)
592	—	2.2 (−7)	1045	—	6.6 (−7)
599	O(III)	3.0 (−6)	1063	S(IV)	1.3 (−6)
609	Mg(X)	1.8 (−5)	1068	—	1.6 (−6)
616	O(II)	4.3 (−7)	1077	S(III)	2.6 (−6)
625	Mg(X)	7.7 (−6)	1085	N(II)	7.9 (−6)
629	O(V)	5.3 (−5)	1122	Si(IV)	5.1 (−6)
639	Ca(VII)	3.6 (−7)	1128	Si(IV)	5.1 (−6)
644	O(II)	4.6 (−7)	1134	N(I)	2.7 (−6)
649	—	1.2 (−7)	1139	Al(XI), Ne(VI)	1.2 (−5)
657	S(IV)	4.0 (−7)	1148	—	3.1 (−6)
661	S(IV)	1.1 (−6)	1152	O(I)	3.9 (−6)
671	N(II)	2.3 (−7)	1157	C(II)	4.3 (−6)
681	Na(IX)	1.4 (−6)	1175	C(III)	3.8 (−5)
685	N(III)	2.8 (−6)	1190	Si(II)	2.2 (−6)
692	—	2.5 (−7)	1194	Si(II)	6.9 (−6)
694	Na(IX)	5.4 (−7)	1199	N(I)	1.1 (−5)
703	O(III)	8.1 (−6)	1206	Si(III)	6.9 (−5)
707	—	9.5 (−7)	1215	H(I)	8.5 (−3)
712	S(VI)	2.7 (−7)	1238	N(V)	1.3 (−5)
718	O(II)	16.0 (−6)	1242	N(V)	1.1 (−5)
728	S(III)	1.9 (−7)	1309	Si(II)	1.7 (−5)
736	Mg(IX)	3.2 (−7)	1277	C(I)	4.0 (−6)
744	S(IV)	4.8 (−7)	1302	O(I)	3.1 (−5)
750	S(IV)	8.7 (−7)	1305	O(I)	8.0 (−5)
760	O(V)	3.4 (−6)	1264	Si(II)	7.1 (−6)
764	N(III), N(IV)	8.1 (−6)	1329	C(I)	6.4 (−6)
770	Ne(VIII)	6.2 (−6)	1335	C(II)	1.3 (−4)
775	N(II)	3.0 (−7)	1351	—	8.3 (−6)
780	Ne(VIII)	3.0 (−6)	1356	O(I)	7.3 (−6)
787	O(IV)	8.2 (−6)	1393	S(IV)	3.5 (−5)

* Doublet.

$R \sim 10$ to 40 and no larger plages. Such conditions occur routinely near solar minimum and sporadically at other times.

By "active," we mean $R \sim 100$, but no flares present. An "active" Sun is typical around solar maximum.

X-ray data come from a variety of satellite and rocket measurements. At the shorter wavelengths, we rely heavily on Wende's 1972 recalibration of earlier data. Culhane et al. (1969) and Kreplin and Horan (1969) also provide some data. Figure 4 shows these results for 1 to 11 Å and presents our adopted values for the active, moderate, and quiet Sun.

For wavelengths longer than 20 Å, we use Freeman and Jones (1970), Argo et al. (1970), Manson (1972), and Malinovski and Heroux (1973). Figure 5 shows the results.

Solar Constant

Table 5 presents the results of this section in the form of solar irradiance averaged over small wavelength intervals. Figure 6 depicts much of the same information; here, however, we include several short wavelength curves to indicate the effect of solar activity on the flux. Table 6 presents the solar irradiance data in the X-ray and EUV regions for the four conditions indicated in figure 6.

The total solar constant (quiet Sun) that we derive is 1357.826 W/m² at 1 AU (1.947 cal/cm² · min). A comparison of this value with previously derived values as presented in NASA Space Vehicle Design Criteria Report SP–8005 (1971) is made in table 7. Note that our value is toward the upper end of the high-altitude results and near the lower end of the ground-based results.

VARIATIONS DUE TO SOLAR ACTIVITY

Solar flux variations fall into natural categories determined by their time scales. Flares have the shortest life times—of the order of minutes. The slowly varying component encompasses changes over hours to days and is due to the appearance, development, and disappearance of active regions. Closely related to this is the 27-day period, which results from the reappearance of active regions as the Sun rotates. Finally, the 11-yr cycle reflects the correlation of all solar activity with the sunspot cycle.

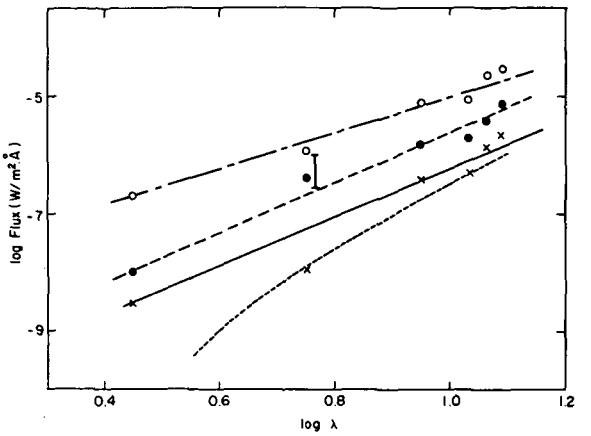

FIGURE 4.—Solar irradiance in the X-ray region. Open circles are Wende's (1972) active Sun, filled circles are his moderate Sun, and x's are his quiet Sun. Lines through the data are the adopted fits. The vertical bar is from Kreplin and Horan (1969) at a time of moderate activity. The dashed line toward the bottom is from Culhane et al. (1969) for an extremely quiet Sun.

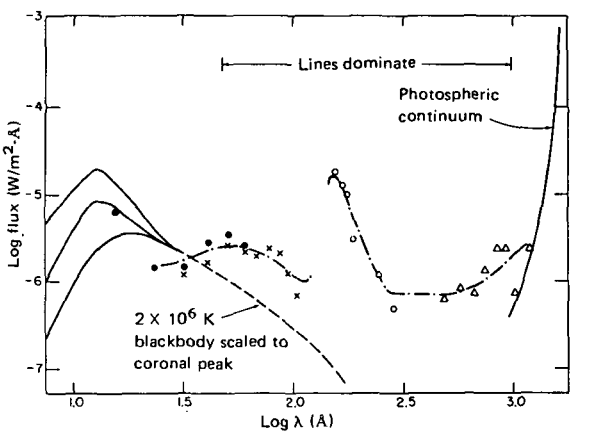

FIGURE 5.—Solar irradiance in the UV and X-ray regions. The solid line to the left is from figure 4; solid line to right is from Nicolas (1973); filled and open circles are from Freeman and Jones (1970); x's are from Manson (1972); and the open triangles are various OSO results. The dash-dotted line is an arbitrary fit.

Flares

We start our discussion with the shortest lived and most energetic phenomena: flares. Flares are traditionally observed in (and, in fact, are defined by) the enhancement of the H_α radiation, even though flux increases are frequently proportionally

TABLE 5.—*Summary of the Quiet Sun Solar Irradiance at All Wavelengths*

Wavelength range, Å	Solar irradiance,[a] W/m²		Percent	Wavelength range, Å	Solar irradiance,[a] W/m²		Percent
	Per Ångstrom	Sum[b]			Per Ångstrom	Sum[b]	
2 to 3	1.8 (−9)	1.8 (−9)	0.000	2400 to 2500	6.42 (−3)	2.51	0.185
3 to 4	5.6 (−9)	7.4 (−9)	.000	2500 to 2600	9.05 (−3)	3.42	.252
4 to 5	2.0 (−8)	2.7 (−8)	.000	2600 to 2700	2.10 (−2)	5.52	.406
5 to 6	5.0 (−8)	7.7 (−8)	.000	2700 to 2800	2.04 (−2)	7.56	.557
6 to 7	1.0 (−7)	1.8 (−7)	.000	2800 to 2900	2.90 (−2)	1.05 (+1)	.770
7 to 8	1.8 (−7)	3.6 (−7)	.000	2900 to 3000	5.24 (−2)	1.57 (+1)	1.156
8 to 9	3.2 (−7)	6.8 (−7)	.000	3000 to 3100	5.18 (−2)	2.09 (+1)	1.538
9 to 10	5.6 (−7)	1.24 (−6)	.000	3100 to 3200	6.35 (−2)	2.72 (+1)	2.005
10 to 11	8.0 (−7)	2.04 (−6)	.000	3200 to 3300	7.81 (−2)	3.50 (+1)	2.580
11 to 12	1.12 (−6)	3.16 (−6)	.000	3300 to 3400	9.00 (−2)	4.40 (+1)	3.243
12 to 13	1.78 (−6)	4.94 (−6)	.000	3400 to 3500	8.94 (−2)	5.30 (+1)	3.902
13 to 14	2.24 (−6)	7.18 (−6)	.000	3500 to 3600	9.49 (−2)	6.25 (+1)	4.601
14 to 15	2.64 (−6)	9.82 (−6)	.000	3600 to 3700	10.51 (−2)	7.30 (+1)	5.375
15 to 20	9.55 (−6)	5.76 (−5)	.000	3700 to 3800	10.40 (−2)	8.34 (+1)	6.141
20 to 30	4.57 (−6)	1.03 (−4)	.000	3800 to 3900	9.45 (−2)	9.28 (+1)	6.836
30 to 40	3.47 (−6)	1.38 (−4)	.000	3900 to 4000	11.34 (−2)	1.04 (+2)	7.672
40 to 50	3.80 (−6)	1.76 (−4)	.000	4000 to 4100	16.31 (−2)	1.20 (+2)	8.873
50 to 60	4.17 (−6)	2.18 (−4)	.000	4100 to 4200	17.00 (−2)	1.37 (+2)	10.125
60 to 70	3.39 (−6)	2.52 (−4)	.000	4200 to 4300	16.59 (−2)	1.54 (+2)	11.347
70 to 80	2.69 (−6)	2.79 (−4)	.000	4300 to 4400	16.72 (−2)	1.71 (+2)	12.578
80 to 90	3.09 (−6)	3.09 (−4)	.000	4400 to 4500	19.28 (−2)	1.90 (+2)	13.998
90 to 100	2.46 (−6)	3.34 (−4)	.000	4500 to 4600	20.06 (−2)	2.10 (+2)	15.475
100 to 110	1.29 (−6)	3.47 (−4)	.000	4600 to 4700	19.86 (−2)	2.30 (+2)	16.938
110 to 120	7.1 (−7)	3.54 (−4)	.000	4700 to 4800	19.89 (−2)	2.50 (+2)	18.403
120 to 130	Near 0	3.54 (−4)	.000	4800 to 4900	18.88 (−2)	2.69 (+2)	19.793
130 to 140	Near 0	3.54 (−4)	.000	4900 to 5000	19.56 (−2)	2.88 (+2)	21.234
140 to 150	1.41 (−6)	3.68 (−4)	.000	5000 to 5100	19.02 (−2)	3.07 (+2)	22.635
150 to 160	1.70 (−6)	3.85 (−4)	.000	5100 to 5200	18.31 (−2)	3.26 (+2)	23.983
160 to 170	1.41 (−6)	3.99 (−4)	.000	5200 to 5300	18.59 (−2)	3.44 (+2)	25.352
170 to 180	1.82 (−6)	4.17 (−4)	.000	5300 to 5400	19.17 (−2)	3.63 (+2)	26.764
180 to 190	1.29 (−6)	4.30 (−4)	.000	5400 to 5500	18.56 (−2)	3.82 (+2)	28.131
190 to 200	1.00 (−6)	4.40 (−4)	.000	5500 to 5600	18.41 (−2)	4.00 (+2)	29.487
200 to 250	3.16 (−6)	5.98 (−4)	.000	5600 to 5700	18.28 (−2)	4.19 (+2)	30.833
250 to 300	1.26 (−6)	6.61 (−4)	.000	5700 to 5800	18.34 (−2)	4.37 (+2)	32.184
300 to 350	2.00 (−6)	7.61 (−4)	.000	5800 to 5900	18.08 (−2)	4.55 (+2)	33.515
350 to 500	7.9 (−7)	8.80 (−4)	.000	5900 to 6000	17.63 (−2)	4.73 (+2)	34.814
500 to 600	6.9 (−7)	9.49 (−4)	.000	6000 to 6100	17.41 (−2)	4.90 (+2)	36.096
600 to 700	9.1 (−7)	1.04 (−3)	.000	6100 to 6200	17.05 (−2)	5.07 (+2)	37.351
700 to 800	7.8 (−7)	1.12 (−3)	.000	6200 to 6300	16.58 (−2)	5.24 (+2)	38.573
800 to 900	1.53 (−6)	1.27 (−3)	.000	6300 to 6400	16.37 (−2)	5.40 (+2)	39.778
900 to 1000	2.52 (−6)	1.52 (−3)	.000	6400 to 6500	15.99 (−2)	5.56 (+2)	40.956
1000 to 1100	2.82 (−6)	1.80 (−3)	.000	6500 to 6600	15.20 (−2)	5.71 (+2)	42.075
1100 to 1200	1.26 (−6)	1.93 (−3)	.000	6600 to 6700	15.55 (−2)	5.87 (+2)	43.220
1200 to 1300	8.71 (−5)	1.06 (−2)	.001	6700 to 6800	15.16 (−2)	6.02 (+2)	44.337
1300 to 1400	4.47 (−6)	1.11 (−2)	.001	6800 to 6900	14.89 (−2)	6.17 (+2)	45.433
1400 to 1500	5.62 (−6)	1.16 (−2)	.001	6900 to 7000	14.50 (−2)	6.31 (+2)	46.501
1500 to 1600	1.05 (−5)	1.27 (−2)	.001	7000 to 7100	14.16 (−2)	6.46 (+2)	47.544
1600 to 1700	1.78 (−5)	1.45 (−2)	.001	7100 to 7200	13.85 (−2)	6.59 (+2)	48.564
1700 to 1800	7.96 (−5)	2.24 (−2)	.002	7200 to 7300	13.56 (−2)	6.73 (+2)	49.562
1800 to 1900	1.63 (−4)	3.86 (−2)	.003	7300 to 7400	13.16 (−2)	6.86 (+2)	50.532
1900 to 2000	4.00 (−4)	7.86 (−2)	.006	7400 to 7500	12.84 (−2)	6.99 (+2)	51.478
2000 to 2100	1.10 (−3)	1.89 (−1)	.014	7500 to 7600	12.65 (−2)	7.12 (+2)	52.409
2100 to 2200	4.69 (−3)	6.58 (−1)	.048	7600 to 7700	12.36 (−2)	7.24 (+2)	53.320
2200 to 2300	6.41 (−3)	1.30	.096	7700 to 7800	12.07 (−2)	7.36 (+2)	54.209
2300 to 2400	5.72 (−3)	1.87	.138	7800 to 7900	11.83 (−2)	7.48 (+2)	55.080

TABLE 5.—*Summary of the Quiet Sun Solar Irradiance at All Wavelengths*—Continued

Wavelength range, Å	Solar irradiance,[a] W/m[2] Per Ångstrom	Sum[b]	Percent	Wavelength range, Å	Solar irradiance,[a] W/m[2] Per Ångstrom	Sum[b]	Percent
7900 to 8000	11.61 (−2)	7.59 (+2)	55.935	50 to 60 × 10[4]	2.73 (−8)	1.36 (+3)	100.000
8000 to 8100	11.36 (−2)	7.71 (+2)	56.771	60 to 70 × 10[4]	1.39 (−8)	1.36 (+3)	100.000
8100 to 8200	11.04 (−2)	7.82 (+2)	57.585	70 to 80 × 10[4]	7.83 (−9)	1.36 (+3)	100.000
8200 to 8300	10.75 (−2)	7.93 (+2)	58.376	80 to 90 × 10[4]	4.74 (−9)	1.36 (+3)	100.000
8300 to 8400	10.51 (−2)	8.03 (+2)	59.150	90 to 100 × 10[4]	3.04 (−9)	1.36 (+3)	100.000
8400 to 8500	10.06 (−2)	8.13 (+2)	59.891	10 to 11 × 10[5]	2.04 (−9)	1.36 (+3)	100.000
8500 to 8600	9.86 (−2)	8.23 (+2)	60.617	11 to 12 × 10[5]	1.42 (−9)	1.36 (+3)	100.000
8600 to 8700	9.68 (−2)	8.33 (+2)	61.330	12 to 13 × 10[5]	1.01 (−9)	1.36 (+3)	100.000
8700 to 8800	9.47 (−2)	8.42 (+2)	62.028	13 to 14 × 10[5]	7.46 (−10)	1.36 (+3)	100.000
8800 to 8900	9.24 (−2)	8.51 (+2)	62.708	14 to 15 × 10[5]	5.61 (−10)	1.36 (+3)	100.000
8900 to 9000	9.20 (−2)	8.61 (+2)	63.386	15 to 16 × 10[5]	4.30 (−10)	1.36 (+3)	100.000
9000 to 9100	8.98 (−2)	8.70 (+2)	64.047	16 to 17 × 10[5]	3.35 (−10)	1.36 (+3)	100.000
9100 to 9200	8.74 (−2)	8.78 (+2)	64.691	17 to 18 × 10[5]	2.65 (−10)	1.36 (+3)	100.000
9200 to 9300	8.57 (−2)	8.87 (+2)	65.322	18 to 19 × 10[5]	2.12 (−10)	1.36 (+3)	100.000
9300 to 9400	8.41 (−2)	8.95 (+2)	65.941	19 to 20 × 10[5]	1.72 (−10)	1.36 (+3)	100.000
9400 to 9500	8.23 (−2)	9.04 (+2)	66.547	20 to 30 × 10[5]	7.28 (−11)	1.36 (+3)	100.000
9500 to 9600	8.06 (−2)	9.12 (+2)	67.141	30 to 40 × 10[5]	1.80 (−11)	1.36 (+3)	100.000
9600 to 9700	7.89 (−2)	9.20 (+2)	67.722	40 to 50 × 10[5]	6.89 (−12)	1.36 (+3)	100.000
9700 to 9800	7.73 (−2)	9.27 (+2)	68.291	50 to 60 × 10[5]	3.23 (−12)	1.36 (+3)	100.000
9800 to 9900	7.56 (−2)	9.35 (+2)	68.848	60 to 70 × 10[5]	1.73 (−12)	1.36 (+3)	100.000
9900 to 10 000	7.39 (−2)	9.42 (+2)	69.392	70 to 80 × 10[5]	1.01 (−12)	1.36 (+3)	100.000
10 to 11 × 10[3]	6.82 (−2)	1.01 (+2)	74.417	80 to 90 × 10[5]	6.34 (−13)	1.36 (+3)	100.000
11 to 12 × 10[3]	5.58 (−2)	1.07 (+2)	78.530	90 to 100 × 10[5]	4.18 (−13)	1.36 (+3)	100.000
12 to 13 × 10[3]	4.64 (−2)	1.11 (+2)	81.943	10 to 11 × 10[6]	2.84 (−13)	1.36 (+3)	100.000
13 to 14 × 10[3]	3.85 (−2)	1.15 (+2)	84.777	11 to 12 × 10[6]	2.00 (−13)	1.36 (+3)	100.000
14 to 15 × 10[3]	3.23 (−2)	1.18 (+2)	87.154	12 to 13 × 10[6]	1.46 (−13)	1.36 (+3)	100.000
15 to 16 × 10[3]	2.67 (−2)	1.21 (+2)	89.118	13 to 14 × 10[6]	1.08 (−13)	1.36 (+3)	100.000
16 to 17 × 10[3]	2.14 (−2)	1.23 (+2)	90.697	14 to 15 × 10[6]	8.24 (−14)	1.36 (+3)	100.000
17 to 18 × 10[3]	1.75 (−2)	1.25 (+3)	91.983	15 to 16 × 10[6]	6.38 (−14)	1.36 (+3)	100.000
18 to 19 × 10[3]	1.44 (−2)	1.26 (+3)	93.042	16 to 17 × 10[6]	5.02 (−14)	1.36 (+3)	100.000
19 to 20 × 10[3]	1.20 (−2)	1.28 (+3)	93.923	17 to 18 × 10[6]	4.01 (−14)	1.36 (+3)	100.000
20 to 30 × 10[3]	5.53 (−3)	1.33 (+3)	97.998	18 to 19 × 10[6]	3.24 (−14)	1.36 (+3)	100.000
30 to 40 × 10[3]	1.53 (−3)	1.35 (+3)	99.125	19t o 20 × 10[6]	2.65 (−14)	1.36 (+3)	100.000
40 to 50 × 10[3]	5.71 (−4)	1.35 (+3)	99.546	20 to 30 × 10[6]	1.16 (−14)	1.36 (+3)	100.000
50 to 60 × 10[3]	2.54 (−4)	1.35 (+3)	99.733	30 to 40 × 10[6]	3.07 (−15)	1.36 (+3)	100.000
60 to 70 × 10[3]	1.32 (−4)	1.36 (+3)	99.830	40 to 50 × 10[6]	1.17 (−15)	1.36 (+3)	100.000
70 to 80 × 10[3]	7.56 (−5)	1.36 (+3)	99.886	50 to 60 × 10[6]	5.49 (−16)	1.36 (+3)	100.000
80 to 90 × 10[3]	4.64 (−5)	1.36 (+3)	99.920	60 to 70 × 10[6]	2.92 (−16)	1.36 (+3)	100.000
90 to 100 × 10[3]	3.01 (−5)	1.36 (+3)	99.942	70 to 80 × 10[6]	1.71 (−16)	1.36 (+3)	100.000
10 to 11 × 10[4]	2.02 (−5)	1.36 (+3)	99.957	80 to 90 × 10[6]	1.07 (−16)	1.36 (+3)	100.000
11 to 12 × 10[4]	1.40 (−5)	1.36 (+3)	99.967	90 to 100 × 10[6]	7.03 (−17)	1.36 (+3)	100.000
12 to 13 × 10[4]	9.97 (−6)	1.36 (+3)	99.975	10 to 11 × 10[7]	4.86 (−17)	1.36 (+3)	100.000
13 to 14 × 10[4]	7.30 (−6)	1.36 (+3)	99.980	11 to 12 × 10[7]	3.48 (−17)	1.36 (+3)	100.000
14 to 15 × 10[4]	5.47 (−6)	1.36 (+3)	99.984	12 to 13 × 10[7]	2.57 (−17)	1.36 (+3)	100.000
15 to 16 × 10[4]	4.18 (−6)	1.36 (+3)	99.987	13 to 14 × 10[7]	1.94 (−17)	1.36 (+3)	100.000
16 to 17 × 10[4]	3.25 (−6)	1.36 (+3)	99.990	14 to 15 × 10[7]	1.49 (−17)	1.36 (+3)	100.000
17 to 18 × 10[4]	2.56 (−6)	1.36 (+3)	99.992	15 to 16 × 10[7]	1.17 (−17)	1.36 (+3)	100.000
18 to 19 × 10[4]	2.05 (−6)	1.36 (+3)	99.993	16 to 17 × 10[7]	9.29 (−18)	1.36 (+3)	100.000
19 to 20 × 10[4]	1.66 (−6)	1.36 (+3)	99.994	17 to 18 × 10[7]	7.49 (−18)	1.36 (+3)	100.000
20 to 30 × 10[4]	7.03 (−7)	1.36 (+3)	99.999	18 to 19 × 10[7]	6.11 (−18)	1.36 (+3)	100.000
30 to 40 × 10[4]	1.72 (−7)	1.36 (+3)	99.999	19 to 20 × 10[7]	5.04 (−18)	1.36 (+3)	100.000
40 to 50 × 10[4]	6.16 (−8)	1.36 (+3)	100.000				

[a] Numbers in parentheses indicate the power of 10 by which the irradiance values given must be multiplied.

[b] Sum of the irradiance at this wavelength interval plus that at all shorter wavelengths.

[c] Sum of the irradiance occurring at this wavelength interval and at shorter wavelengths as a percent of the total irradiance.

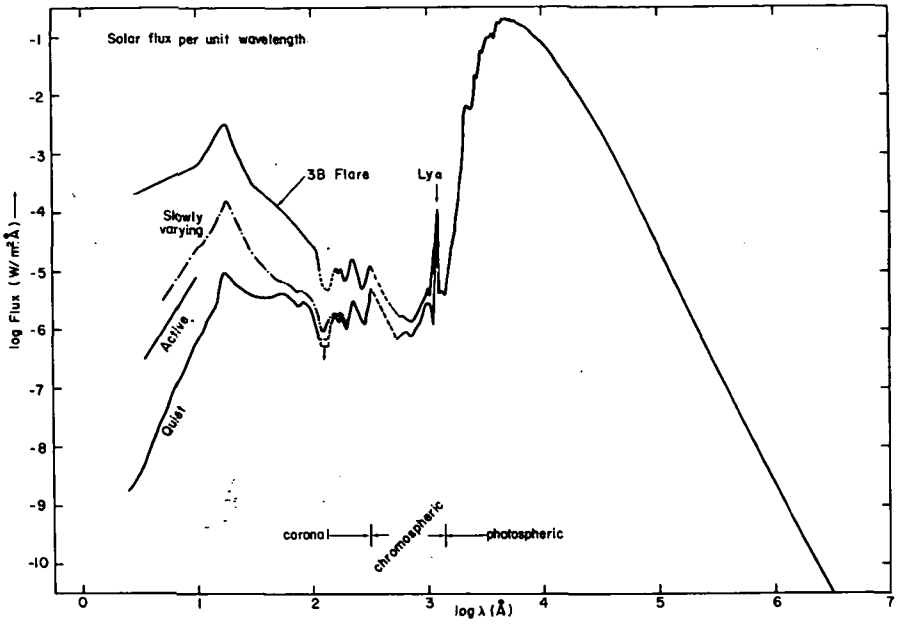

FIGURE 6.—Summary of solar irradiance at all wavelengths.

TABLE 6.—*Summary of Solar Irradiance for the Quiet Sun, a Typical Active Sun, the Maximum Enhancement Due to the Slowly Varying Component, and an Importance 3B Flare*

Wavelength range, A	Solar irradiance,[a] W/m²							
	Quiet Sun		Active Sun		Slowly varying Sun		3B flare	
	Per Angstrom	Sum[b]	Per Angstrom	Sum[b]	Per Angstrom	Sum[b]	Per Angstrom	Sum[b]
2 to 3	1.8 (−9)	1.8 (−9)	1.5 (−7)	1.5 (−7)	4.5 (−7)	4.5 (−7)	1.78 (−4)	1.78 (−4)
3 to 4	5.6 (−9)	7.4 (−9)	4.0 (−7)	5.5 (−7)	1.26 (−6)	1.71 (−6)	2.34 (−4)	4.12 (−4)
4 to 5	2.0 (−8)	2.7 (−8)	8.3 (−7)	1.38 (−6)	2.40 (−6)	4.11 (−6)	3.16 (−4)	7.28 (−4)
5 to 6	5.0 (−8)	7.7 (−8)	1.58 (−6)	2.96 (−6)	3.71 (−6)	7.82 (−6)	3.64 (−4)	1.09 (−3)
6 to 7	1.0 (−7)	1.8 (−7)	2.51 (−6)	5.47 (−6)	6.30 (−6)	1.41 (−5)	4.17 (−4)	1.51 (−3)
7 to 8	1.8 (−7)	3.6 (−7)	3.80 (−6)	9.27 (−6)	1.00 (−5)	2.41 (−5)	4.78 (−4)	1.99 (−3)
8 to 9	3.2 (−7)	6.8 (−7)	6.02 (−6)	1.53 (−5)	1.41 (−5)	3.82 (−5)	5.25 (−4)	2.51 (−3)
9 to 10	5.6 (−7)	1.24 (−6)	7.95 (−6)	2.32 (−5)	2.34 (−5)	6.16 (−5)	5.89 (−4)	3.10 (−3)
10 to 11	8.0 (−7)	2.04 (−6)	1.12 (−5)	3.44 (−5)	2.82 (−5)	8.98 (−5)	6.31 (−4)	3.73 (−3)
11 to 12	1.12 (−6)	3.16 (−6)	1.41 (−5)	4.85 (−5)	3.71 (−5)	1.27 (−4)	1.00 (−3)	4.73 (−3)
12 to 13	1.78 (−6)	4.94 (−6)	1.78 (−5)	6.63 (−5)	4.47 (−5)	1.32 (−4)	1.26 (−3)	5.99 (−3)
13 to 14	2.24 (−6)	7.18 (−6)	1.90 (−5)	8.53 (−5)	6.31 (−5)	2.35 (−4)	1.78 (−3)	7.77 (−3)
14 to 15	2.64 (−6)	9.82 (−6)	2.00 (−5)	1.05 (−4)	7.94 (−5)	3.14 (−4)	2.24 (−3)	1.00 (−2)
15 to 20	9.55 (−6)	5.76 (−5)	2.40 (−5)	2.25 (−4)	1.58 (−4)	1.10 (−3)	3.16 (−3)	2.58 (−2)
20 to 30	4.57 (−6)	1.03 (−4)	1.02 (−5)	3.27 (−4)	3.24 (−5)	1.43 (−3)	5.13 (−4)	3.09 (−2)
30 to 40	3.47 (−6)	1.38 (−4)	6.17 (−6)	3.89 (−4)	1.18 (−5)	1.54 (−3)	2.04 (−4)	3.30 (−2)
40 to 50	3.80 (−6)	1.76 (−4)	5.63 (−6)	4.45 (−4)	8.51 (−6)	1.63 (−3)	1.59 (−4)	3.46 (−2)
50 to 60	4.17 (−6)	2.18 (−4)	5.37 (−6)	4.99 (−4)	6.92 (−6)	1.70 (−3)	1.09 (−4)	3.57 (−2)
60 to 70	3.39 (−6)	2.52 (−4)	4.37 (−6)	5.43 (−4)	5.49 (−6)	1.76 (−3)	7.08 (−5)	3.64 (−2)
70 to 80	2.69 (−6)	2.79 (−4)	3.22 (−6)	5.75 (−4)	4.17 (−6)	1.80 (−3)	4.68 (−5)	3.68 (−2)
80 to 90	3.09 (−6)	3.09 (−4)	3.80 (−6)	6.13 (−4)	4.68 (−6)	1.84 (−3)	4.57 (−5)	3.73 (−2)
90 to 100	2.46 (−6)	3.34 (−4)	2.88 (−6)	6.42 (−4)	3.63 (−6)	1.88 (−3)	3.09 (−5)	3.76 (−2)
100 to 110	1.29 (−6)	3.47 (−4)	1.48 (−6)	6.57 (−4)	1.91 (−6)	1.90 (−3)	1.44 (−5)	3.77 (−2)
110 to 120	7.1 (−7)	3.54 (−4)	7.9 (−7)	6.64 (−4)	1.02 (−6)	1.91 (−3)	7.08 (−6)	3.78 (−2)
120 to 130	Near 0	3.54 (−4)	Near 0	6.64 (−4)	Near 0	1.91 (−3)	Near 0	3.78 (−2)

TABLE 6.—*Summary of Solar Irradiance for the Quiet Sun, a Typical Active Sun, the Maximum Enhancement Due to the Slowly Varying Component, and an Importance 3B Flare*—Continued

Wavelength range, Å	Solar irradiance,[a] W/m²							
	Quiet Sun		Active Sun		Slowly varying Sun		3B flare	
	Per Ångstrom	Sum[b]	Per Ångstrom	Sum[b]	Per Ångstrom	Sum[b]	Per Ångstrom	Sum[b]
130 to 140	Near 0	3.54 (−4)	Near 0	6.64 (−4)	Near 0	1.91 (−3)	Near 0	3.78 (−2)
140 to 150	1.41 (−6)	3.68 (−4)	1.41 (−6)	6.79 (−4)	1.95 (−6)	1.93 (−3)	1.10 (−5)	3.79 (−2)
150 to 160	1.70 (−6)	3.85 (−4)	1.70 (−6)	6.96 (−4)	2.29 (−6)	1.95 (−3)	1.23 (−5)	3.81 (−2)
160 to 170	1.41 (−6)	3.99 (−4)	1.41 (−6)	7.10 (−4)	1.91 (−6)	1.97 (−3)	9.32 (−6)	3.81 (−2)
170 to 180	1.82 (−6)	4.17 (−4)	1.82 (−6)	7.28 (−4)	2.45 (−6)	2.00 (−3)	1.15 (−5)	3.83 (−2)
180 to 190	1.29 (−6)	4.30 (−4)	1.29 (−6)	7.41 (−4)	1.70 (−6)	2.01 (−3)	7.10 (−6)	3.83 (−2)
190 to 200	1.00 (−6)	4.40 (−4)	1.00 (−6)	7.51 (−4)	1.32 (−6)	2.03 (−3)	5.62 (−6)	3.84 (−2)
200 to 250	3.16 (−6)	5.98 (−4)	3.16 (−6)	9.09 (−4)	4.07 (−6)	2.23 (−3)	1.58 (−5)	3.92 (−2)
250 to 300	1.26 (−6)	6.61 (−4)	1.26 (−6)	9.72 (−4)	1.58 (−6)	2.31 (−3)	5.25 (−6)	3.94 (−2)
300 to 350	2.00 (−6)	7.61 (−4)	2.00 (−6)	1.07 (−3)	6.17 (−6)	2.62 (−3)	1.77 (−5)	4.00 (−2)
350 to 500	7.9 (−7)	8.80 (−4)	7.9 (−7)	1.19 (−3)	9.6 (−7)	2.76 (−3)	4.47 (−6)	4.07 (−2)
500 to 600	6.9 (−7)	9.49 (−4)	6.9 (−7)	1.26 (−3)	8.1 (−7)	2.84 (−3)	1.55 (−6)	4.09 (−2)
600 to 700	9.1 (−7)	1.04 (−3)	9.1 (−7)	1.35 (−3)	1.07 (−6)	2.95 (−3)	1.77 (−6)	4.10 (−2)
700 to 800	7.8 (−7)	1.12 (−3)	7.8 (−7)	1.43 (−3)	9.1 (−7)	3.04 (−3)	1.38 (−6)	4.12 (−2)
800 to 900	1.53 (−6)	1.27 (−3)	1.53 (−6)	1.58 (−3)	1.70 (−6)	3.21 (−3)	3.24 (−6)	4.15 (−2)
900 to 1000	2.52 (−6)	1.52 (−3)	2.52 (−6)	1.83 (−3)	2.82 (−6)	3.49 (−3)	4.78 (−6)	4.20 (−2)
1000 to 1100	2.82 (−6)	1.80 (−3)	2.82 (−6)	2.12 (−3)	3.09 (−6)	3.80 (−3)	5.01 (−6)	4.25 (−2)
1100 to 1200	1.26 (−6)	1.93 (−3)	1.26 (−6)	2.24 (−3)	1.35 (−6)	3.94 (−3)	1.62 (−6)	4.26 (−2)
1200 to 1300	8.71 (−5)	1.06 (−2)	8.71 (−5)	1.09 (−2)	9.34 (−5)	1.33 (−2)	1.07 (−4)	5.33 (−2)
1300 to 1400	4.47 (−6)	1.11 (−2)	4.47 (−6)	1.14 (−2)	4.77 (−6)	1.37 (−2)	5.02 (−6)	5.38 (−2)

[a] Numbers in parentheses indicate the power of 10 by which the irradiance values given must be multiplied.
[b] Sum of the irradiance at this wavelength interval plus that at all shorter wavelengths.

TABLE 7.—*Comparison of Our Value for the Solar Constant With Other Values*

Source	Solar constant, W/m²
Our value	1358
Ground-based measurements:	
Nicolet, 1951	1380
Aldrich and Hoover, 1952	1352
Stair and Johnston, 1954	1428
Johnson, 1954	1395
Allen, 1958	1380
Gast, 1965	1390
Stair and Ellis, 1968	1369
Labs and Neckel, 1968	1365
Makarova and Kharitonov, 1969	1418
High-altitude measurements:	
Thekaekara, 1970 (various instruments)	1352
	1349
	1343
	1358
	1338
Murcray, 1969	1338
Kondratyev and Nikolsky, 1970	1353
Drummond and Hickey, 1968	1360
Plamondon, 1969	1353

higher for X-rays and for the far UV. The coincidence of H_α flares with short wavelength radiation enhancements is by no means one to one. While many investigators have found a strong correlation of H_α flares with X-ray bursts, some X-ray bursts may be associated with other short-lived chromospheric phenomena such as active prominences (Hoover, Thomas, and Underwood, 1972).

Optical flares are classified according to the area and brightness of the H_α radiation. Table 8 summarizes this classification system. The frequency of occurrence depends on the phase of the 11-yr solar sunspot cycle; flares are most numerous during sunspot maximum. During solar maximum flares of importance 1 or greater appear on the average every 2 to 2½ hr. For X-ray bursts, Drake's (1971) analysis yields approximately the same figure, as his threshold of detection was at a value typical of an importance 1 flare.

Smith and Booton (1961) found that approximately 79 percent of all flares of importance 1 or

greater are of importance 1; 19 percent are of importance 2, and about 2 percent are of importance 3 or greater. The proportion of high importance flares should probably be revised downward, however, on the basis of new data and more reliable classifications (Dodson and Hedeman, 1971). These proportions vary little, if any, with phase of the solar sunspot cycle (Smith, 1962).

Small, low importance flares occur in far greater abundance than the large bright importance 3 or 4 flares. Small events (subflares or other chromospheric events that may trigger X-ray emission) are even more prolific, especially during solar maximum. Good statistics on these are not available. Undoubtedly the lower the threshold, the larger the number of events. We do not concern ourselves unduly with small events, as the fluxes involved are not substantial; however, they may be of use as predictors of larger events.

Any average figures on flare occurrence are, however, somewhat misleading, for some active regions are far more flare productive than others. Frequently several major flares occur within a few days out of the same active region. An outstanding example of such a multiple series of events is represented by the August 1972 flares. Furthermore, one solar cycle may be far more flare productive than another. Cycle 19 (1954 to 1963) produced 77 proton flares, but cycle 20 produced less than half as many.

Nor can we use the sunspot number to predict frequency of flare occurrence. Major flares are less closely correlated with sunspot number than are lesser flares. Because the major flares are responsible for the most dramatic variations in flux, this makes it virtually impossible to predict X-ray flux in terms of the sunspot number, except on the most general statistical basis. To make matters even worse, the cycle for major events, such as proton flares, may be doubly peaked, with the second maximum occurring during the decline of the sunspot cycle (Gnevyshev, 1967). The resurgence of activity represented by the August 1972 flares in cycle 20 is quite analogous to the postmaximum phase of activity in cycles 17, 18, and 19 (Dodson and Hedeman, 1973).

To further complicate the attempt to give a figure for the frequency of occurrence of major flares, it is now apparently accepted that proton flare producing regions are not distributed randomly in solar longitude. (See the section entitled "The 27-Day Period.") The distribution of sunspots, however, does not unambiguously portray such a nonrandom organization.

TABLE 8.—*Definition of Importance Classes Flares*

Importance	Area (solar hemisphere)
S	Less than 10^{-4}
1	1.0 to 2.5 × 10^{-4}
2	2.5 to 6.0 × 10^{-4}
3	6.0 to 12 × 10^{-4}
4	More than 12 × 10^{-4}

TABLE 9.—*Frequency of Occurrence of Flares as a Function of Importance and Phase of the Solar Cycle*

Year (after maximum)	Flares per day			
	Importance			
	3	2	1	Total
0	0.050	1.0	9.0	10
1	.045	.9	8.0	9
2	.035	.7	7.3	8
3	.015	.3	2.7	3
4	.010	.2	1.8	2
5	.005	.1	.9	1
6	.002	.05	.5	.5
7	.001	.01 to .05	.1 to .5	.1 to .5
8	.005	.1	.9	1
9	.025	.5	4.5	5
10	.045	.9	8.0	9

All these qualifications should be kept in mind when interpreting table 9, which summarizes our knowledge of the frequency of flares over the sunspot cycle. Most of the data used to prepare table 9 come from Smith and Smith (1963) and Dodson and Hedeman (1971). We now examine in further detail the characteristics of flares in several wavelength intervals.

Characteristically, soft X-ray bursts have a rise time close to 4 min, and a decay time of 12 min (Drake, 1971). Many bursts have a superimposed short impulsive phase, of 1- or 2-min duration; occurring near the start of the flare. For hard X-rays (~ 1Å or shorter) this phase consists of numbers of even shorter spikes with time scales from under 1 s up to 10 s. The impulsive phase dominates increasingly with hardening of the X-rays (Frost, 1969). Another way of stating this is that the hardness of the X-rays decreases with time after

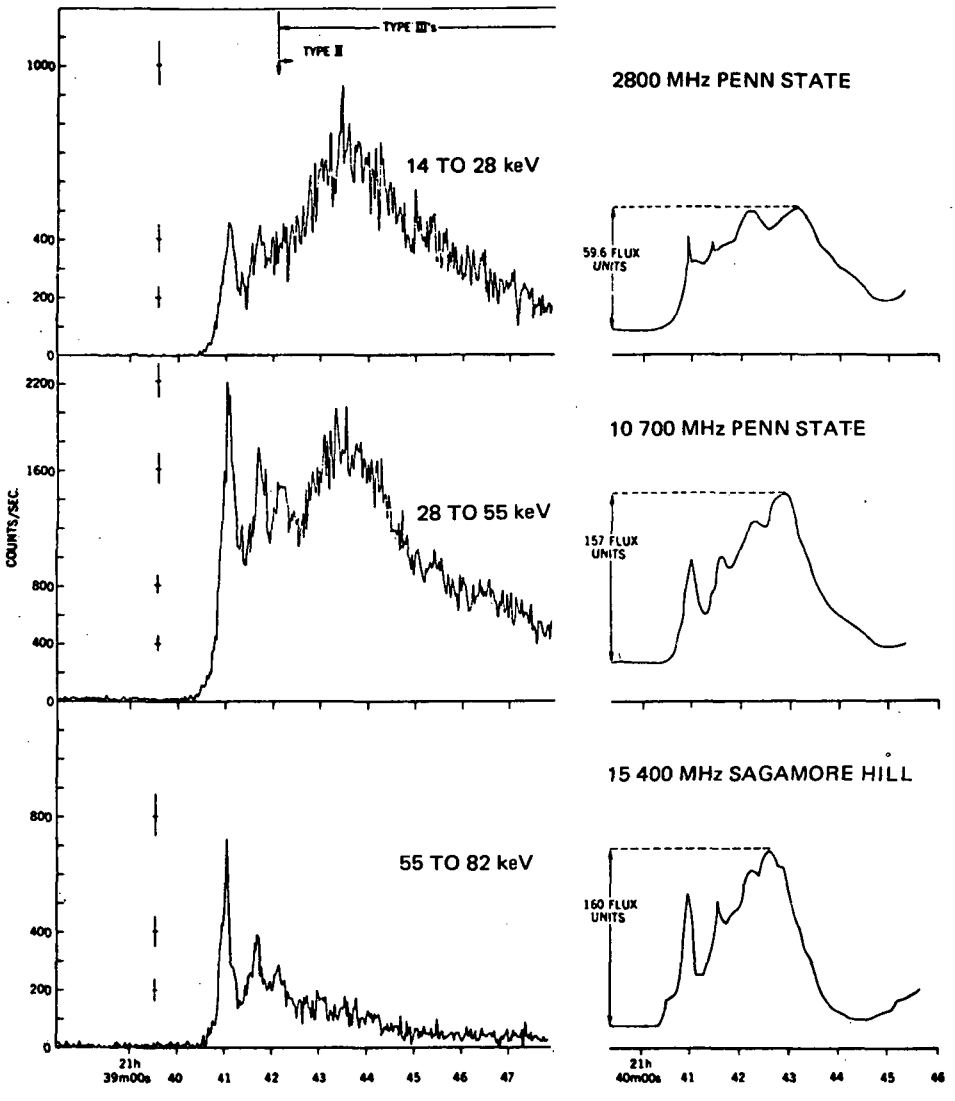

FIGURE 7.—X-ray spectrum of a solar flare at three wavelengths (from Frost, 1969).

the onset of an event. Figure 7 is an example of an X-ray event at several wavelengths.

The relationship between soft X-ray peak flux (2 to 20 Å) and H_α flare importance classification has been ambiguous, for there are large deviations from the mean relation between them. Nevertheless, analyses of significant numbers of flares (Drake, 1971; Hoover, Thomas, and Underwood, 1972) point to the existence of such a relationship, particularly with the brightness of the H_α flare (Krieger et al., 1972) as opposed to its area. Large deviation from the mean correlation may be partly explained by the fact that the X-ray flux is also affected by the general level of solar activity and nature of the plage region in which the flare occurs (Hoover et al., 1972). In general, though, we may state that large, bright H_α flares frequently produce large X-ray fluxes. Small flares never produce large X-ray bursts. Conversely, strong X-rays are always accompanied by some H_α event, though it may occur behind the solar limb (implying a coronal origin for the X-rays).

We obtain typical soft X-ray peak fluxes in large flares from the data of Dere et al. (1973), who used the NRL Solrad 10 satellite to observe the series of large flares in August 1972. These

TABLE 10.—*Summary of Wende's (1972) Data on X-Ray Flux From Solar Flares*

Flare type	log flux, W/m² − Å Wavelength, Å		
	2.5	6.5	16
1N	−5.8	−5.7	−5.0
1B	−5.0	−4.7	−4.5
2B	−4.6	−4.4	−4.4
3B	−3.5	−3.2	−3.0
Quiet	−8.5	−6.8	−5.5

data also provide useful information on the fluxes of smaller flares. Table 10 presents the results. Although coronal emission lines between 2 and 20 Å arising from highly ionized ions are very greatly enhanced during a flare, most of the contribution to the flux in this spectral region is due to the continuum (Neupert, 1971).

From 20 to 1400 Å, emission lines dominate the spectrum. Unfortunately, we are not aware of any published data on overall EUV enhancements at the time of major flares, and it is of course risky to extrapolate. The estimated enhancement and fluxes in table 6 are based on extrapolations, using the enhancement in the X-ray wavelengths, Hall's (1971) measurements of several emission lines, and Heath's (1969) measurements at H(I) Lyman-alpha (1216 Å) and longer wavelengths.

For the EUV line emission from 300 to 1400 Å, the enhancement varies widely from one line to another, depending on the ionization potential and the wavelength. Highly ionized ions are present but weak in the quiet Sun spectrum. During flares, the integrated emission in these lines from the entire Sun increases by a factor of 2 or 3 (Neupert, 1967). Chromospheric lines show considerable enhancement over the flare area (Hall, 1971; Wood and Noyes, 1972), but when the small fraction of the solar disk covered by the flares is taken into account, the total enhancement only amounts to about 1 to 2 percent for a subflare, 10 percent or less for an importance 1 flare, and 25 to 50 percent for an importance 2 flare.

Hall (1971) found an empirical relationship between the enhancement of EUV lines in terms of H_α flare areas, namely $E \propto kA^{3/2}$, where A is the H_α flare area and k is a constant of proportionality that ranges from less than 0.4 for H(I), HE(I), and some coronal lines to 2.4 and 2.8 for chromospheric lines like Si(III) ($\lambda = 1206$) and O(VI) ($\lambda = 1032$). Caution must be exercised in using this relationship, however, for it is based on relatively little data and does not allow for the large known differences between flares.

The two types of flares discussed in the section on X-rays exist in the EUV as well (Kelly and Rense, 1972). The impulsive EUV events are associated with the impulsive nonthermal X-ray events (Wood and Noyes, 1972). The time of maximum for such events is nearly the same at all wavelengths (Wood et al., 1972). Time scales run around 2 min.

The gradual EUV burst is associated with the gradual thermal X-ray bursts (Wood and Noyes, 1972). The time of maximum in the EUV is about 1 or 2 min before the X-ray or H_α maximum (Hall, 1971; Wood et al., 1972). Time scales are around 5 to 10 min.

Lyman-alpha radiation of H(I) is, of course, the strongest line in the EUV and is treated separately from the general EUV flux, though the data are surprisingly sparse. The profile shown in figure 8 is a quiet Sun profile from Bruner and Rense (1969). Measurements by Heath (1973) and Hall (1971) indicate an overall enhancement from the entire disk in Lyman-alpha of 16 to 18 percent for an importance 3 flare.

At longer wavelengths the enhancement due to flares becomes negligible. Heath (1969) observed a 3B flare on April 21, 1969, with intermediate band filters centered around 1800 and 2950 Å. Any enhancement was less than 1 percent.

Note that only a small fraction of even the brightest H_α flares are known to be visible in white light. DeMastus and Stover (1967) measured the white light enhancement of a band centered around 5800 Å during a 3B flare. They found a 16-percent enhancement in a small kernel covering around 10^{-5} of the solar surface. Using these data, we estimate maximum enhancements in the visual and near IR (4000 to 12 500 Å) to be about 10^{-5} to 10^{-6} for even major flares. Nevertheless, three absorption lines in the visible spectrum are affected sufficiently to warrant mention: H_α and the H and K lines of Ca(II).

Zirin and Tanaka (1973) measured the H_α flux for the August 4 and August 7, 1972, importance 3B flares and found total energies of 2.0 ×

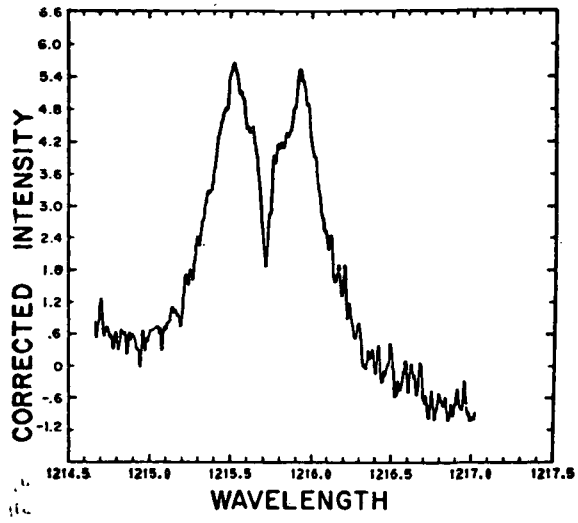

FIGURE 8.—The profile of the Lyman-alpha line (from Bruner and Rense, 1969).

10^{30} and 2.5×10^{30} ergs. These figures are an order of magnitude lower than previous estimates for similar flares. The authors attribute the discrepancy to the fact that earlier estimates assumed that the wide line widths and high central intensities prevailed over the entire area of the flare and for most of its lifetime. These observations show that much of the H_α emission is concentrated into bright, short-lived kernels and that the excessive line width (12 Å or more) occurs only in these kernels. The energies of Zirin and Tanaka (1973) represent a H_α total disk enhancement of about 0.1 percent in the central 1-Å passband, where the emission may be as great as three times the local continuum (Jefferies et al., 1954; Smith and Smith, 1963). It is much less, of course, in the neighboring wavelengths.

The *H* and *K* lines of Ca(II) ($\lambda \sim 390$ Å) are also enhanced in flares. We can only estimate the enhancement in the lines on the basis of flare line profile information (for example, Smith and Smith, 1963). Peak intensities may exceed the local continuum by a factor of 3 within 1 Å of the line center. The whole disk enhancement is then about 0.5 percent.

The Slowly Varying Component (Nonperiodic)

The term "slowly varying component" was originally used to refer to the day-to-day changes of the solar radio flux. The radio emission responsible for the overall increased flux was identified with regions lying above chromospheric plages. These plages are best observed in the visual as areas of enhanced H_α or Ca(II) *K*-line emission. X-rays and UV radiation exhibit variations similar to those in the radio region, hence the term "slowly varying component" has been applied to these radiations also. The entire volume encompassing visual, X-ray and radio plage; enhanced magnetic fields; sunspots; and coronal enhancements constitutes an "active region."

A rapid rise in flux and a slow decay characterizes the slowly varying component, as it does all solar activity, from flares to the 11-yr cycle. An active region may last as long as several solar rotations, but its most active phase is early in its life.

According to Sawyer (1968), the increase in total visible solar radiation due to a single plage is minuscule, amounting to about 0.1 percent; however, it may be as much as 100 percent in certain EUV emission lines and 50 percent at radio frequencies. The major effect of a plage, however, occurs for X-rays. As a rule, the shorter the wavelengths, the greater the amplitude.

SOLRAD data (Friedman and Kreplin, 1969; Kreplin, 1970) extend over several years and are ideal for studying variations on a time scale from hours to months. In March 1966, near solar minimum, there was only a single active region on the solar disk; thus it was possible to ascertain the flux enhancement caused by one typical active region. Kreplin (1970) found that the overall solar flux increased by a factor of 100 in the 0- to 8-Å range and a factor of 50 in the 8- to 20-Å band as the region rotated into view on the solar disk.

Typical month-to-month variations due to the slowly varying component would be a factor of 15 at 16 Å and a factor of 1.7 at 50 Å (Kreplin, 1970). We might expect, occasionally, factors of 100 at 5 Å. The month-to-month variation will be greatest during the rise to and decline from maximum of the solar cycle. During minimum, the scarcity and weakness of active regions prevent large variations; during maximum, the large number of active regions present forces a statistical "constancy" on the total flux.

In addition to the variations caused by the

appearance and disappearance of active regions as the Sun rotates, the slowly varying component also includes a contribution due to the development of an active region. For example, Krieger et al. (1972) found an increase of a factor of 20 in a 4-hr period at 10 Å, while Kreplin (1970) reported a similar decrease over 2 days at 16 Å. Both of these variations were due to changes in the structure of an active region.

The amplitude of enhancements in the EUV is far less, down to a factor 1.5 at 50 Å (Hall and Hinteregger, 1970), 1.1 at 1350 Å, 1.05 at 1700 Å (Heath, 1973). At longer wavelengths, there is probably no substantial variation, based on an extrapolation of Heath's (1969) flare data. Because this region is dominated by line rather than continuum emission, the strengthening of a few strong lines plays a major role.

Reeves and Parkinson (1972) find that typical chromospheric lines (with excitations up to about that of Fe(X)) vary about 10 percent. Chapman and Neupert (1974) also find a 10-percent average variability for lines from 140 to 400 Å for a change of 10-cm flux corresponding to quiet to active. They would increase this to 20 percent for the shorter wavelength lines. The variations for Lyman is of the order of 30 percent (Vidal-Madjar et al., 1973).

In strong contrast, the total flux from the high ionization lines of Fe(XVI) (λ=335 Å) and Fe(XV) (λ=284 Å) change by a factor of 4 because of the appearance or disappearance of an active region (Neupert, 1967). These lines arise from the high temperature, 2 million degree corona as opposed to the 10 000° to 15 000° chromosphere and chromosphere/corona interface where the lower ionization lines originate.

Figure 9 shows the peak variations observed as a function of wavelength based mainly on the SOLRAD data. Note that the slowly varying component falls approximately midway between the 3B flare curve and Wende's (1972) "typical active Sun."

In the visual region, the largest fluctuations occur in the *H* and *K* lines of Ca(II). On the basis of the increased Ca(II) *K*-line emission in plages, which is, on the average, 20 percent of the continuum (Smith, 1960), and the area of a plage (up to half a percent of the disk), one can estimate that the overall enhancement in the line cores due to an active region may be at most 5 percent.

The Mg(II) lines at 2803 and 2795 Å behave very similar to the Ca(II) lines; Fregda (1971) found a correlation coefficient of 0.92 between the intensities of the Mg(II) *K* line (λ=2795) and the Ca(II) *K* line. The emission cores are far more pronounced in the Mg(II) lines than the

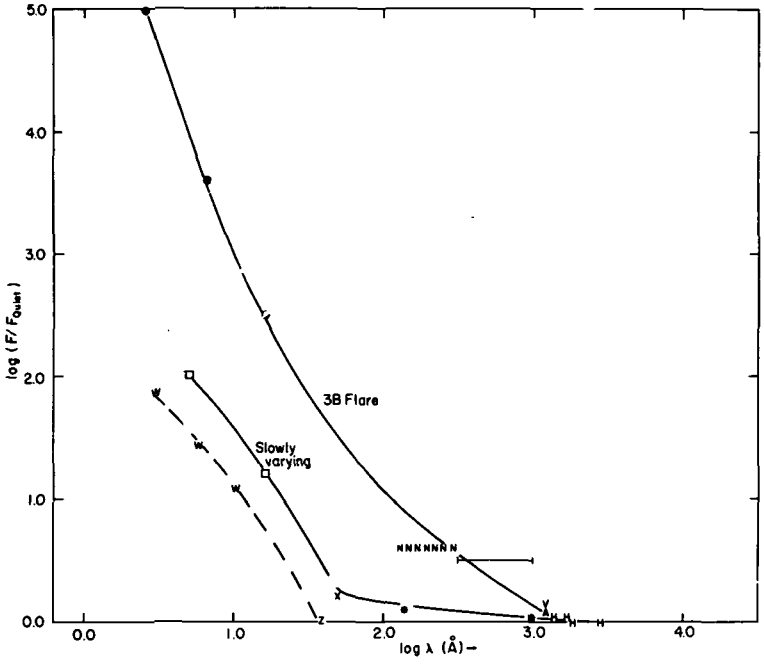

FIGURE 9.—Variations in the solar irradiance as a function of wavelength. (Filled circles: Dere et al., 1973; horizontal bar: Hall, 1971; *V*: Vidal-Madjar et al., 1973; *A*: Heath, 1969, Lyman-alpha; *H*: Heath, 1973; open squares: Kreplin, 1970; *X*: Hall and Hinteregger, 1970; asterisks: Reeves and Parkinson, 1972; *W*: Wende, 1972; *Z*: fig. 5.)

Ca(II) lines, so the percentage enhancement due to active regions is somewhat greater.

As to the visual continuum, we use Rogerson's (1961) work on faculae, the photospheric counterpart of plages. Faculae are only visible near the limb and reach a maximum contrast of facula to photosphere intensity of 1.6 at a heliocentric distance of $\cos \theta = 0.2$. Even for a large facula that would cover 5×10^{-3} of the solar disk when at central meridian, the enhancement is only 0.1 percent.

Variations in any other part of the visible spectrum, including H_α, are dwarfed by those in the *H* and *K* lines, and can safely be ignored. The same is true for the IR. Not until one reaches the radio frequencies do we find that plages make a significant contribution to the overall flux. However, the energies and fluxes at radio radiations are so low as to be insignificant in comparison with the total flux. Radio data are, nevertheless, of great value in diagnosing solar active regions and in estimating the solar flux variations at other wavelengths.

The 27-Day Period

Whereas the slowly varying component is largely due to the growth and decay of active regions, the 27-day period is caused strictly by the rotation of the Sun.

The existence of a 27-day period is quite evident at X-ray wavelengths, but how long it persists *in phase* and what the exact value is for the period, are more difficult questions.

Because a single active region may survive for several rotations, a periodicity in the X-ray (and EUV) flux is produced by its appearance and disappearance around the solar limb. This periodicity would persist only for the active lifetime of the region—no more than three or four rotations. However, new active regions tend strongly to form out of the remnants of old ones (Bumba and Howard, 1965). Consequently, localized activity may extend to perhaps a year or so (Heath, 1969).

The existence of a single 27-day period over longer periods of time depends upon the recurrence of major active regions at, or near, the same longitude over extended time scales. The existence of a correlation of major sunspot groups with solar longitude has been pointed out by numerous writers; for example, Sawyer (1968), Haurwitz (1968), Levitsky (1967), Wilcox and Schatten (1967), Sakurai (1966), Warwick (1965), and Guss (1964). The correlation does not exist for normal-size active regions, spot groups, or flares but appears clearly for the most energetic flares and the largest spot groups and active regions. Haurwitz's data go back the longest (over 100 yr), and she determines a period of 27.213 days, which is slightly shorter than the Carrington period of 27.275 days. Of course, the solar rotation period is a function of latitude and altitude, but the shortness of Haurwitz's period, relative to even the fastest of these, is very interesting.

This correlation does not predict any long-enduring 27-day period for the minimum monthly flux in the EUV or in X-rays but is evidence for a 27-day quasi-periodicity of the very large flares and concurrent strong X-ray bursts, at least over time spans of about 100 yr.

Direct observational evidence for a long-enduring 27-day period is limited, but studies of up to a couple of years' duration have been reported in the X-ray region by Teske (1971*a*, *b*) and Parkinson and Pounds (1971). Radio emission is also known to follow a 27-day period.

The amplitude of the 27-day period can be inferred directly from the data presented in the section entitled "The Slowly Varying Component (Nonperiodic)" because the cause of the periodicity is the appearance and disappearance of active regions around the solar limb.

TABLE 11.—*Factors for the Conversion of Mean Irradiance to Irradiance at Any Given Day*[a]

Day	Factor
Jan. 1	0.9669
Feb. 1	.9710
Mar. 1	.9819
Apr. 1	.9988
May 1	1.0155
June 1	1.0284
July 1	1.0337
Aug. 1	1.0304
Sept. 1	1.0189
Oct. 1	1.0024
Nov. 1	.9851
Dec. 1	.9722

[a] To convert, divide mean irradiance by these numbers.

The 1-Year Period

The varying distance of Earth from the Sun over its orbit is cause for a substantial variation in the solar flux. Table 11 presents appropriate factors by which one should multiply the fluxes to correct to a certain time of year. The following sine curve approximation (day: April 4) for this factor is proportional to the solar distance squared and is accurate to within 0.3 percent at all times:

$$r^2 = 1.0004 + 0.0334 \sin$$

Note that for near UV, visible, and IR wavelengths, this variation swamps those due to flares, the slowly varying component, and the 27-day and 11-yr cycles.

The 11-Year Cycle

The 11-yr sunspot cycle is defined in terms of the periodicity in the number of sunspots and spot groups. The Wolf number, or Zurich number, R is a function of a combination of the total number of spots and the number of spot groups:

$$R = K(10g + f)$$

where K is a personal factor to bring all measurements to the same scale, g is the number of groups, and f is the number of spots. A closely related datum is the sunspot area (for example, see Tandberg-Hanssen, 1967), which varies in phase with R.

Actually, the polarity of the leading spot in a group changes from one cycle to the next, leading to the designation of a "22-yr" sunspot cycle. There is little reason to believe that the polarity flip affects any other parameter of the 11-yr "subcycle." However, the overall solar magnetic field changes polarity in a similar manner. Thus, the solar and terrestrial magnetic fields are alternately parallel and antiparallel for alternate 11-yr cycles.

Successive solar maximums differ quite considerably. It has been suggested that alternate maxima have higher R values, but this is by no means clear cut. The International Geophysical Year solar maximum of cycle 19 turned out to be unique in that it was exceptionally active. Because this was a well-studied maximum, much of the data obtained there are often assumed to be typical of all solar maxima. Caution should be exercised because of the uniqueness of the activity during this period.

The sunspot number is the most easily measured index of solar activity and, in fact, has been traced back to the mid-18th century.

The question is sometimes raised whether the presence of a large number of sunspots measurably decreases the solar flux in the visible portion of the spectrum. It is therefore instructive to make some estimates.

An extremely large sunspot may have an umbral area of 6×10^{-4} of the solar disk. The intensity may be as low as a tenth of the photospheric intensity at 500 Å (Zwaan, 1968). The total reduction in flux from such a sunspot is therefore well below 0.1 percent. One can argue that a more realistic estimate must take into account the fact that at solar maximum there are many spots on the solar surface. When the Zurich sunspot R number is 200, the total *area* of all the sunspots is of the order of 4×10^{-3} (using upper limits; for example, see Tandberg-Hanssen, 1967). If one makes the extreme assumption that this whole area is umbra at a tenth the photospheric intensity, one still only obtains a diminution of 0.4 percent of the total solar flux. Actually, only about one-sixth of the sunspot area is umbra, for the larger fraction is the penumbral contribution, with an intensity of about 0.7 the photospheric intensity. So we again arrive at the result that sunspots cause at most a 0.1-percent fluctuation in visible flux. Furthermore, brightening in the plage region near large spot groups will make up for part of this deficiency.

Many laymen, and even scientists in related fields, attribute certain effects to sunspots that should properly be attributed to flares or other aspects of solar activity. This confusion arises, in large part from the fact that the cycle of solar activity is closely associated with the sunspot cycle. For example, the number and area of Ca(II) or H_α plage regions are closely related to the sunspot number. Similarly, the correlations with R number of He(II)(λ=304) flux; nonflare X-ray flux at all spectral wavelengths; and radio emission, especially at 10 cm; are very good.

It seems safe to conclude that the 11-yr cycle in X-rays, for example, is *largely* due to the variation in the number of active regions.

There is a strong indication, however, that superimposed on this phenomenon is a variation of X-ray and EUV emissions from similar active regions over the 11-yr solar sunspot cycle (Kreplin, 1970; Parkinson and Pounds, 1971). This is in the sense that emission tends to be greater near solar maximum. An explanation may lie in the higher coronal densities observed near solar maximum, which could amplify the effects of any solar activity present, especially at X-ray wavelengths.

It should be emphasized that the importance and intensity of flares correlates only poorly with sunspot number; therefore, data from such correlations should be used only in the broadest statistical manner.

Kreplin (1970) reports SOLRAD satellite data for the period 1964 to 1969. Solar minimum in the X-rays occurred around July 1964 when the flux at 50 Å was about 2×10^{-6} W/m^2 · Å and the flux at 16 Å was below threshold intensity for the experiment ($<2 \times 10^{-8}$ W/m^2 · Å); Van Gils and DeGraaff (1967) have similar data. Maximum occurred in mid-1970 with the monthly minimum 16-Å flux at that time 25 percent higher than in 1968 or in 1971 (Horan and Kreplin, 1972).

Gibson and Van Allen (1970) used Explorer 33 and 35 measurements to demonstrate a 150-percent rise at 10 Å from July 1966 to December 1968. Using Culhane et al. (1969) to scale the data from one wavelength to another, we find that there should have been another 50 percent rise at 10 Å from December 1968 until maximum in 1970. July 1966 probably presented conditions not too different from minimum.

For cycle 20, the monthly minimum flux at 10 Å probably rose about 225 percent from minimum to maximum; at 16 Å, the rise was probably about 125 percent.

Allowing for some rise from 1964 to 1966 (previously ignored), and the fact that cycle 20 had a rather low maximum, we estimate that monthly minima will vary by a factor of 3 to 5 at 10 Å and 2 to 3 at 16 Å, from solar minimum to solar maximum.

At longer wavelengths, we have only correlations of fluxes with such things as R and the 10-cm flux to go by in determining the amplitude of variation over the 11-yr cycle. As we stated previously, these correlations are very imperfect. The major emission line strengths have been correlated with R. The flux from the He(II) line at 304 Å, for example, increases by 15 percent as R goes from 50 to 200 (Timothy and Timothy, 1970). This is typical of solar minimum to maximum behavior. Vidal-Madjar et al. (1973) report an identical result for Lyman-alpha. Hinteregger (1970) does his correlations with 10-cm flux and gets similar results for other chromospheric lines; however, high excitation coronal lines may vary by a factor of 5 to 10 more.

In the visible regions, no measurements have been made over extended time periods. However, observations of similar stars have failed to turn up any variations (limiting accuracy about 1 percent) over times of about 20 yr. We conclude that, at wavelengths greater than 1500 Å or so, there is no variation over the 11-yr solar sunspot cycle.

Longer Periods

Periodic variations in the solar flux over time scales greater than 11 yr can, for the most part, only be indirectly deduced, as no accurate astronomical observations were made until well into the 20th century. Further, we restrict ourselves to astronomical data in this paper and have not considered geological data to any extent.

Because sunspot numbers are, however, available for several hundred years, some authors have analyzed them for long-term periodicity. If such periods exist, there *may* be a similar period in solar flux, especially for X-rays.

Numerous analyses of the sunspot number for an 80-yr period have been done. Kopecky (1962) reviews some of these. More recently, Hartmann (1971) has used untreated, unsmoothed R values from 1700 to 1950. By plotting alternate cycles as positive and negative, he obtains a convincing portrayal of an 80-yr cycle in R. The most recent maximum was in 1950. The amplitude of variation is about 100 in the R number at solar maximum.

Longer-period cycles have been suggested (for example, Henkel, 1972), but the evidence for them is necessarily very weak.

A curious periodicity deduced from the R numbers by Shapiro and Ward (1962) with a 25- to 26-month period may provide an example of the

confusion of cause and effect. Shapiro and Ward's power spectrum of the R numbers showed a small, but according to them significant, peak at around 25 to 26 months. This coincides with a similar periodicity for the strength of the stratospheric winds (Veryard and Ebdon, 1961) and other terrestrial phenomenon (Heath, 1973). It has been suggested that the variation in the winds might be due to the sunspot number periodicity (for example, Westcott, 1964); however, it seems more likely to us that the sunspot number periodicity is the result of the varying photographic quality of images of the solar disk caused by the atmospheric changes.

The 26 000-Yr Period

The procession of Earth's orbit with a period of 26 000 yr produces a change in the amount of solar energy received at a given terrestrial latitude. Currently, perihelion occurs very near the middle of the northern hemisphere winter; in 13 000 yr this situation will be reversed.

Long-Term Secular Changes

While we have omitted theoretical arguments from most of this paper, it seems appropriate to mention that models of stellar evolution, borne out by observations of star clusters, indicate that the Sun has been brightening and getting slightly hotter over the past 5 billion years and will continue to brighten (at near constant temperature) for the next 4 billion years. The rate of brightening is about 1 percent in 50 million years and the rate of solar effective temperature rise has been about 1 K per 25 million years.

ACKNOWLEDGMENT

This study was supported in part by NASA Grant NGL 21–002–033.

REFERENCES

Aldrich, L. B., and W. H. Hoover, 1952, *Science,* **116,** p. 3.
Allen, C. W., 1958, *J. Roy. Meteorol. Soc.,* **84,** p. 307.
Argo, H. V., J. A. Bergey, and W. D. Evans, 1970, *Astrophys. J.,* **160,** p. 283.
Arvesen, J. C., R. N. Griffen, and B. D. Pearson, Jr., 1969, *Appl. Opt.,* **8,** p. 2215.
Bonnet, R. M., and J. E. Blamont, 1968, *Solar Phys.,* **3,** p. 64.
Broadfoot, A. L., 1972, *Astrophys. J.,* **173,** p. 681.
Bruckner, G., and K. Nicolas, 1973, private communication, Naval Research Lab., Washington, D.C.
Bruner, E. C., Jr., and W. A. Rense, 1969, *Astrophys. J.,* **157,** p. 417.
Bumba, V., and R. Howard, 1965, *Astrophys. J.,* **142,** p. 796.
Carver, J. H., B. H. Horton, G. W. A. Lockey, and B. Rofe, 1972, *Solar Phys.,* **27,** p. 347.
Chapman, R. D., and W. M. Neupert, 1974, *J. Geophys. Res.,* **79,** p. 4138.
Culhane, J. L., P. W. Sanford, M. L. Shaw, K. J. H. Phillips, A. P. Willmore, P. J. Bowen, K. A. Pounds, and D. G. Smith, 1969, *Mon. Nat. Roy. Astron. Soc.,* **145,** p. 435.
David, K. H., and G. Elste, 1962, *Z. Astrophys.,* **54,** p. 12.
DeMastus, H. L., and R. P. Stover, 1967, *Publ. Astron. Soc. Pac.,* **79,** p. 615.
Dere, K. P., D. M. Horan, and R. W. Kreplin, 1973, World Data Center A Report **UAG–28,** p. 298.
Dodson, H. W., and E. R. Hedeman, 1971, World Data Center A Report **UAG–14.**
Dodson, H. W., and E. R. Hedeman, 1973, World Data Center A Report **UAG–28,** p. 16.
Donnelly, R. F., and J. H. Pope, 1973, National Oceanic and Atmospheric Administration Tech. Rep. ERL 276–SEL 25.
Drake, J. F., 1971, *Solar Phys.,* **16,** p. 152.
Drummond, A. J., and J. R. Hickey, 1968, *Solar Energy,* **12,** p. 217.
Drummond, A. J., J. R. Hickey, W. J. Scholes, and E. G. Laue, 1968, *Nature,* **218,** p. 259.
Dupree, A. K., M. C. E. Huber, R. W. Noyes, W. H. Parkinson, E. M. Reeves, and G. L. Withbroe, 1973, *Astrophys. J.,* **182,** p. 321.
Dupree, A. K., and E. M. Reeves, 1971, *Astrophys. J.,* **165,** p. 599.
Eddy, J. A., P. J. Lena, and R. M. MacQueen, 1969, *Solar Phys.,* **10,** p. 330.
Farmer, C. B., and S. J. Todd, 1964, *Appl. Opt.,* **3,** p. 453.
Freeman, F. F., and B. B. Jones, 1970, *Solar Phys.,* **15,** p. 288.
Fregda, K., 1971, *Solar Phys.,* **21,** p. 60.
Friedman, H., and R. W. Kreplin, 1969, *Ann. IQSY,* **3,** p. 78.
Frost, K. J., 1969, *Astrophys. J. Lett.,* **158,** p. 159.
Gast, P. R., 1965, *Handbook of Geophysics and Space Environment,* McGraw-Hill Book Co. Inc.
Gibson, J. G., and J. A. Van Allen, 1970, *Astrophys. J.,* **161,** p. 1135.
Gingerich, O., R. W. Noyes, W. Kalkofen, and Y. Cuny, 1971, *Solar Phys.,* **18,** p. 347.
Gnevyshev, M. N., 1967, *Solar Phys.,* **1,** p. 107.
Guss, D., 1694, *Phys. Rev. Lett.,* **13,** p. 363.
Hall, L. A., 1971, *Solar Phys.,* **21,** p. 167.

Hall, L. A., and H. E. Hinteregger, 1970, *J. Geophys. Res.*, **75**, p. 6959.
Hartmann, R., 1971, *Solar Phys.*, **21**, p. 246.
Haurwitz, M., 1968, *Astrophys. J.*, **151**, p. 351.
Heath, D. F., 1969, *J. Atmos. Sci.*, **26**, p. 1157.
Heath, D. F., 1973, *J. Geophys. Res.*, **78**, p. 2779.
Henkel, R., 1972, *Solar Phys.*, **25**, p. 498.
Hinteregger, H. E., 1970, *Ann. Geophys.*, **26**, p. 547.
Holweger, H., 1967, *Z. Astrophys.*, **65**, p. 365.
Hoover, R. B., R. J. Thomas, and J. H. Underwood, 1972, *Adv. Space Sci. Technol.*, **11**.
Horan, D. M., and R. W. Kreplin, 1972, NRL Report 6800.
Jefferies, J. T., E. v. P. Smith, and H. J. Smith, 1954, *Astrophys. J.*, **129**, p. 146.
Johnson, F. S., 1954, *J. Meteorol.*, **11**, p. 431.
Kelly, P. T., and W. A. Rense, 1972, *Solar Phys.*, **26**, p. 431.
Kondratyev, K. Ya., and G. A. Nikolsky, 1970, *Quart. J. Roy. Meteorol. Soc.*, **96**, p. 509.
Kopecky, M., 1962, *Bull. Astron. Inst. Czech.*, **13**, p. 63.
Koutchmy, S., and R. Peyturaux, 1970, *Astro. Astrophys.*, **5**, p. 470.
Kreplin, R. W., 1970, *Ann. Geophys.*, **26**, p. 567.
Kreplin, R. W., and D. M. Horan, 1969, NRL Report 7482.
Krieger, A. S., F. R. Paolini, G. S. Vaiana, and D. Webb, 1972, *Solar Phys.*, **22**, p. 150.
Labs, D., and H. Neckel, 1967, *Z. Astrophys.*, **65**, p. 133.
Labs, D., and H. Neckel, 1968, *Z. Astrophys.*, **69**, p. 1.
Labs, D., and H. Neckel, 1970, *Solar Phys.*, **15**, p. 79.
Laue, E. G., and A. J. Drummond, 1968, *Science*, **161**, p. 888.
Levitsky, L., 1967, *Izv. Krym. Astrofiz. Observ.*, **37**, p. 137.
Linsky, J. L., 1973, *Solar Phys.*, **28**, p. 409.
Makarova, E. A., and A. V. Kharitonov, 1969, *Soviet Astron. AJ*, **12**, p. 599.
Malinovsky, M., and L. Heroux, 1973, *Astrophys. J.*, **181**, p. 1009.
Manson, J. E., 1972, *Solar Phys.*, **27**, p. 107.
Murcray, D. G., 1969, Univ. of Denver Report, AFCRL-69-0070.
Murcray, F. H., D. G. Murcray, and W. J. William, 1964, *Appl. Opt.*, **3**, p. 1373.
NASA Space Vehicle Design Criteria, 1971, "Solar Electromagnetic Radiation," NASA SP-8005.
Neupert, W. N., 1967, *Solar Phys.*, **2**, p. 294.
Neupert, W. N., 1971, *Physics of the Solar Corona*, C. J. Macris, ed., Springer-Verlag, New York.
Nicolas, K., 1973, private communication.
Nicolet, M., 1951, *Ann. Astrophys.*, **14**, p. 249.
Noyes, R. W., and W. Kalkofen, 1970, *Solar Phys.*, **15**, p. 120.
Parkinson, W. H., and K. A. Pounds, 1971, *Solar Phys.*, **17**, p. 146.
Parkinson, W. H., and E. M. Reeves, 1969, *Solar Phys.*, **10**, p. 342.
Pierce, A. K., 1954, *Astrophys. J.*, **119**, p. 312.
Plamondon, J. A., 1969, *JPL Space Programs Summary*, **3**, p. 162.
Reeves, E. M., and W. H. Parkinson, 1970, *Astrophys. J. Suppl.* **21**.
Reeves, E. M., and W. H. Parkinson, 1972, Harvard College Observatory Report TR-32.
Rogerson, J. B., 1961, *Astrophys. J.*, **134**, p. 331.
Rottman, G. J., 1973, Laboratory for Atmospheric and Space Physics, Univ. of Colorado, Boulder, Colo., private communication cited in Donnelly and Pope, 1973.
Saiedy, F., 1960, *Mon. Nat. Roy. Astron. Soc.*, **121**, p. 483.
Saiedy, F., and R. M. Goody, 1959, *Mon. Nat. Roy. Astron. Soc.*, **119**, p. 213.
Sakurai, K., 1966, *Publ. Astron. Soc. Japan*, **18**, p. 350.
Sawyer, C., 1968, *Ann. Rev. Astron. Astrophys.*, **6**, p. 115.
Shapiro, R., and F. Ward, 1962, *J. Atmos. Sci.*, **19**, p. 506.
Smith, E. v. P., 1960, *Astrophys. J.*, **132**, p. 202.
Smith, H. J., 1962, Geophysics Research Directorate Res. Note, Air Force Cambridge Research Laboratories AFCRL-62-827.
Smith, H. J., and W. D. Booton, 1961, Geophysics Research Directorate Res. Note No. 58, Air Force Cambridge Research Laboratories AFCRL-472.
Smith, H. J., and E. v. P. Smith, 1963, *Solar Flares*, Macmillan Co.
Stair, R., and H. T. Ellis, 1968, *J. Appl. Meteorol.*, **7**, p. 635.
Stair, R., and R. G. Johnston, 1954, *J. Res. Nat. Bur. Stand.*, **57**, p. 205.
Tandberg-Hanssen, E., 1967, *Solar Activity*, Blaisdell Pub. Co., Waltham, Mass.
Teske, R. G., 1971*a*, *Solar Phys.*, **19**, p. 356.
Teske, R. G., 1971*b*, *Solar Phys.*, **21**, p. 146.
Timothy, A. F., and J. G. Timothy, 1970, *J. Geophys. Res.*, **75**, p. 6950.
Thekaekara, M. P., ed., 1970, *The Solar Constant and the Solar Spectrum Measured From a Research Aircraft*, NASA TR R-351.
Van Gils, J. N., and W. DeGraaff, 1967, *Solar Phys.*, **2**, p. 290.
Veryard, R. G., and R. A. Ebdon, 1961, *Meteorol. Mag.*, **90**, p. 125.
Vidal-Madjar, A., J. E. Blamont, and B. Phissamaj, 1973, *J. Geophys. Res.*, **78**, p. 1115.
Warwick, C. S., 1965, *Astrophys. J.*, **141**, p. 500.
Wende, C. D., 1972, *Solar Phys.*, **22**, p. 492.
Westcott, P., 1964, *J. Atmos. Sci.*, **21**, p. 572.
Widing, K. G., J. D. Purcell, and G. D. Sandlin, 1970, *Solar Phys.*, **12**, p. 52.
Wilcox, J., and K. Schatten, 1967, *Astrophys. J.*, **147**, p. 364.
Willstrop, R. V., 1965, *Mem. Roy. Astron. Soc.*, **69**, p. 83.
Withbroe, G., 1970*a*, *Solar Phys.*, **11**, p. 42.

Withbroe, G., 1970*b*, *Solar Phys.*, **11**, p. 208.
Wood, A. T., Jr., and R. W. Noyes, 1972, *Solar Phys.*, **24**, p. 180.
Wood, A. T., Jr., R. W. Noyes, A. K. Dupree, M. C. E. Huber, W. H. Parkinson, E. M. Reeves, and G. L. Withbroe, 1972, *Solar Phys.* **24**, p. 169.
Zirin, H., and K. Tanaka, 1973, *The Flares of August 1972*, Calif. Inst. Tech. Observ. Rep.
Zwaan, C., 1968, *Ann. Rev. Astron. Astrophys.*, **6**, p. 135.

DISCUSSION

RASOOL: Do we understand the mechanism of the 11-yr cycle?

SMITH: There are some who think they understand it, but I think the answer is no, we do not really understand it.

RASOOL: Is there any reason why there should be a 22-yr cycle?

SMITH: The 22-yr cycle occurs because of the change in the polarity. We have the increase in the number of sunspots every 11 yr, but the polarity of the leading sunspots changes with every 11-yr cycle; and so, on that basis, we have a 22-yr cycle. Babcock has presented a model that explains how the magnetic flux lines get twisted, producing the active regions and the rise of the magnetic flux to the surface of the Sun. It breaks through and we see the sunspots and the surrounding magnetic regions that are responsible for the plages.

PRIESTER: Because the radio radiation of the Sun has been left out of this talk, I would like to report some very recent results that have been obtained with the 100-m fully steerable radiotelescope at Bonn, which is located at Effelsberg. The telescope has provided pictures of the Sun measured at a wavelength of 2.8 cm, where we can clearly see beautiful coronal condensations, which are also the source of X-ray radiation. I would like to point out the persistence of these features, even the small features. These data were taken at a time when the Skylab astronauts monitored the Sun, too, on August 30, 1973. Within 24 hr, a fully developed new coronal condensation has appeared right in the center of a very active group of four condensations. Also striking, is the persistence of even the smaller features over longer periods of time; further, we do not find any limb brightening, which should be expected at this wavelength, given the beam size of 1 arcmin. I would like to point out that 30 percent of the observing time with the Bonn radiotelescope has been set aside for foreign guest observers.

SMITH: The variations from one day to the next are, of course, what we would call the slowly varying component that we also find in the X-rays.

QUESTION: Of course, meteorologists have been fascinated by the idea that the solar constant can change, and I thought you said that, in principle, we would get as much as a 2-percent change in the visible. If I misunderstood, what is the maximum that you would guess for the change in the solar constant, the solar activity?

SMITH: This has to be explained. The figure of 2 percent variation applies not to the solar constant or the total visible light. It refers to the total light from the solar disk that is emitted within certain narrow spectral bands, such as the cores of the *K* line of ionized calcium and the H_α line.

MITCHELL: I am a little puzzled by one thing about the solar constant variation. This is something I commented on years ago. If you have a large sunspot crossing the Sun, it has an effect on reducing the photospheric emission from the region of the spot by something like half, as I understand it. This is in the umbra. If the spots are big enough, that figures out to be up to something like one-half percent of the total radiation emitted from the photosphere. Why would it not follow that the radiation in the visible actually is a negative function of sunspot number? How do we know that the rest of the solar disk increases in radiation by an amount that just compensates for the "shadowing" effect, of individual sunspots? I am referring to some statistics on very large sunspots that occurred around 1946 and maybe some other dates. The total areas of all sunspots on the disk can get up to a fraction of a percent during high sunspot maxima.

ROOSEN: Dr. Abbot, whom we honored today, actually did publish a lot of work on the solar constant, and in his publication (Smithsonian Miscellaneous Collections, No. 4545, 1963) the variation in solar constant values that he got over a solar cycle is roughly about two-tenths of a percent, and he did, indeed, also point out that a large sunspot group crossed the central meridian of the Sun, the UV flux did drop substantially. The drop that he published is a little bit larger than I think anyone would believe from observations made in 1920, but he did find that the UV flux (in the sense of ground-based observations, 0.35 μm or so) increased. The UV flux increased with increasing sunspot numbers, but as a large spot crossed the central meridian, the UV flux dropped.

NOYES: I think we will have to agree that these early observations are pioneering ones. It would be very interesting to repeat this with modern equipment.